ON THE NUMERICAL REALIZATION OF THE EMBEDDING DOMAIN TECHNIQUE FOR A CLASS OF SHAPE OPTIMIZATION PROBLEMS

K. KUNISCH AND G. PEICHL

ABSTRACT. An embedding domain technique is proposed to characterize the gradient of shape optimization problems. A discussion of the numerical realization of the arising saddle point problems is given and numerical examples are discussed.

1. INTRODUCTION

In this paper we address some numerical issues related to shape optimization problems that are formulated by means of the embedding domain technique. We focus on the fact that this technique provides an elegant and numerically useful representation of the gradient of the costfunctional with respect to parameters characterizing the admissible domains. By means of examples it is demonstrated that gradients based on the embedding domain technique give reasonable gradient information in cases when finite difference gradients are useless.

Let us briefly describe the contents. Section 2 contains a summary of the primal-dual formulation of the embedding domain technique and gives the infinite dimensional version of the gradient representation. In Section 3 an approximation based on mixed finite elements is discussed. A discussion of the numerical realization of the saddle point problem, arising from the primal-dual formulation, based on the Schur complement is contained in Section 4. In Section 5 we analyze in detail one dimensional problems and a two-dimensional problem for which the exact analytical solution can be constructed. The two main contributions of this section are that

- for the specific method that we propose it is advisable to characterize the gradient first in terms of primal and dual variables

1991 *Mathematics Subject Classification.* 49Q10, 35J20.

Department of Mathematics, University of Graz, Austria, supported in part by Fonds zur Förderung der wissenschaftlichen Forschung, SFB-UF8 Optimization and Control.

and to discretize the optimality system thereafter, rather than discretizing the infinite dimensional optimization problem first and than calculate its derivative,

- no difficulties due to locking effects [HJ, HN] were detected.

2. The infinite dimensional problem and its gradient

In this section we recall the application of an embedding domain technique to a class of shape optimization problems. Let

$$\Omega_\gamma = \{(x,y)\colon \gamma(y) < x < 1, y \in (0,1)\} \quad \text{for } \gamma \in \mathcal{S},$$

denote a family of Lipschitzian domains which is parametrized by the set of feasible shape functions

$$\mathcal{S} = \{\gamma \in H^3(0,1)\colon \mu \le \gamma(y) \le \nu,\ y \in [0,1],\ |\gamma|_{H^3} \le \rho\},$$

for constants $0 < \mu < \nu < 1$ and $\mu < \rho$. The curved part of $\partial\Omega_\gamma$ given by

$$\Gamma_\gamma = \{(\gamma(y), y)\colon y \in (0,1)\}$$

is characterized by γ which acts as the optimization variable. For given $f \in L^2_{loc}(\mathbb{R}^2)$ and $\gamma \in \mathcal{S}$ let $H^1_0(\Omega_\gamma)$ denote the solution of

$$\begin{aligned} -\Delta u &= f \quad \text{in } \Omega_\gamma \\ u &= 0 \quad \text{on } \partial\Omega_\gamma. \end{aligned} \tag{2.1}$$

As model optimization problem we consider the least squares problem

$$(P_\gamma) \qquad \begin{aligned} &\min \int_{\mathcal{C}} |\tau_{\mathcal{C}} u - z|^2 ds \quad \text{over } \gamma \in \mathcal{S} \\ &\text{subject to } u_\gamma \text{ solution to (2.1).} \end{aligned}$$

Here $\mathcal{C}$ denotes a fixed curve in $(\bar\nu, 1) \times (0,1)$, with $\bar\nu \in (\nu, 1)$, $\tau_{\mathcal{C}}$ stands for the trace on $\mathcal{C}$ and $z \in L^2(\mathcal{C})$ represents a measurement or a desired profile of the state along $\mathcal{C}$.

In order to overcome the difficulties due to the varying domains Ω_γ, the partial differential equation (2.1) that appears as a constraint in (P_γ) is realized by an embedding domain formulation. For this purpose we put $\hat\Omega = (0,1) \times (0,1)$ and we introduce the Banach spaces.

$$\hat V = H^1_0(\hat\Omega)$$
$$H^{1/2}_{00}(\Gamma_\gamma) = \{\chi \in L^2(\Gamma_\gamma)\colon \exists \hat v \in \hat V(\tau_\gamma \hat v = \chi)\}$$

endowed with the norms

$$\|\hat v\|^2_{\hat V} = (\nabla \hat v, \nabla \hat v)_{\hat\Omega},$$

and

$$\|\chi\|_{H_{00}^{1/2}(\Gamma_\gamma)} = \inf\{\|\hat{v}\|_{\hat{V}} : \hat{v} \in \hat{V}, \tau_\gamma \hat{v} = \chi\}$$

respectively. Above $\tau_\gamma \in \mathcal{L}(\hat{V}, H_{00}^{1/2}(\Gamma_\gamma))$ denotes the interior trace operator onto Γ_γ. We associate with (2.1) the following system defined on $\hat{\Omega}$:

Find $(\hat{u}_\gamma, \hat{g}_\gamma) \in \hat{V} \times H_{00}^{1/2}(\Gamma_\gamma)^*$ satisfying

$$\begin{cases} (\nabla \hat{u}_\gamma, \nabla \hat{v})_{\hat{\Omega}} - \langle \hat{g}_\gamma, \tau_\gamma \hat{v}\rangle_{\Gamma_\gamma} = (\tilde{f}, \hat{v})_{\hat{\Omega}}, & \text{for all } \hat{v} \in \hat{V}, \\ \tau_\gamma \hat{u} = 0. \end{cases} \tag{2.2}$$

where

$$\tilde{f} = \begin{cases} f & \text{in } \Omega_\gamma, \\ 0 & \text{otherwise}, \end{cases}$$

and $\langle \cdot, \cdot \rangle$ indicates the duality pairing between $H_{00}^{1/2}(\Gamma_\gamma)^*$ and $H_{00}^{1/2}(\Gamma_\gamma)$. Defining the continuous bilinear forms

$$\begin{aligned} &a(\cdot,\cdot) : \hat{V} \times \hat{V} \to \mathbb{R} & &b(\cdot,\cdot) : \hat{V} \times H_{00}^{1/2}(\Gamma_\gamma) \to \mathbb{R}^* \\ &a(\hat{u}, \hat{v}) = (\nabla \hat{u}, \nabla \hat{v})_{\hat{\Omega}} & &b(\hat{v}, \hat{g}) = -\langle \hat{g}, \tau_\gamma \hat{v}\rangle_{\Gamma_\gamma}, \end{aligned}$$

(2.2) becomes a special case of the saddlepoint problem:

Find $(\hat{u}_\gamma, \hat{g}_\gamma) \in \hat{V} \times H_{00}^{1/2}(\Gamma_\gamma)^*$ such that

$$\begin{cases} a(\hat{u}_\gamma, \hat{v}) + b(\hat{v}, \hat{g}_\gamma) = (\tilde{f}, \hat{v}) & \text{for all } \hat{v} \in \hat{V}, \\ b(\hat{u}_\gamma, \hat{w}) = 0 & \text{for all } \hat{w} \in H_{00}^{1/2}(\Gamma_\gamma)^*, \end{cases}$$

which in turn is equivalent to the system

$$\begin{aligned} A\hat{u}_\gamma + \tau_\gamma^* \hat{g}_\gamma &= \tilde{f} \\ \tau_\gamma \hat{u}_\gamma &= 0, \end{aligned} \tag{2.3}$$

where $A \in \mathcal{L}(V, V^*)$ is the operator associated with the bilinear form $a(\cdot,\cdot)$. Since a is $\hat{V}$–elliptic and τ_γ is surjective the existence of a unique solution $(\hat{u}_\gamma, \hat{g}_\gamma)$ to (2.2) follows (see e.g. Theorem 1.1 in [BF]).

To describe the relationship between the solutions to (2.1) and to (2.2) we denote by $\tilde{u}$ the extension by zero to $\hat{\Omega}$ of a function u defined on Ω_γ. Then, if u_γ is a solution to (2.1) the pair $(\tilde{u}_\gamma, \frac{\partial u}{\partial n}|\Gamma_\gamma)$ solves (2.2). Conversely, if $(\hat{u}_\gamma, \hat{g}_\gamma)$ solves (2.2) then $u_\gamma = \hat{u}_\gamma|\Omega_\gamma$ is the solution to (2.1) [KP1]. As a consequence the optimization problem (P_γ) is equivalent to

$$(\hat{P}_\gamma) \qquad \begin{aligned} &\min \int_{\mathcal{C}} |\tau_{\mathcal{C}}\hat{u}_\gamma - z|^2 ds \quad \text{over } \gamma \in \mathcal{S} \\ &\text{subject to } \ (\hat{u}_\gamma, \hat{g}_\gamma) \text{ solution to (2.2).} \end{aligned}$$

The formulation of (P_γ) as $(\hat{P}_\gamma)$ has two advantages over (P_γ). First (P_γ) is formulated over the fixed domain $\hat{\Omega}$ whereas (P_γ) involves the domains Ω_γ which vary with γ, and secondly the embedding domain formulation allows an extremely useful representation of the gradient of the cost functional

$$J(\hat{u}_\gamma) = \int_{\mathcal{C}} |\tau_{\mathcal{C}}\hat{u}_\gamma - z|^2 ds \tag{2.4}$$

with respect to $\gamma \in \mathcal{S}$. For this purpose we introduce the dual system in $\hat{V} \times H^{1/2}_{00}(\Gamma_\gamma)^*$:

$$\begin{cases} (\nabla\hat{\lambda}_\gamma, \nabla\hat{v})_\Omega - \langle \hat{\mu}_\gamma, \tau_\gamma \hat{v}\rangle_{\Gamma_\gamma} = 2 \int\limits_{\mathcal{C}} (\tau_{\mathcal{C}}\hat{u}_\gamma - z)\tau_{\mathcal{C}}\hat{v}\, ds \\ \tau_\gamma\hat{\lambda}_\gamma = 0, \quad \text{for all } \hat{v} \in \hat{V}, \end{cases} \tag{2.5}$$

where $\hat{u}_\gamma$ is the first component of the solution to (2.2). Note that the left hand sides of the primal equation (2.2) and the dual equation (2.5) coincide. The assumptions on $\mathcal{S}$ ensure the existence of g, $\mu \in L^2(0,1)$ such that the representations

$$\begin{aligned} \langle \hat{g}_\gamma, \varphi\rangle_{\Gamma_\gamma} &= \int\limits_0^1 g(y)\varphi(\gamma(y), y)\sqrt{1+\dot{\gamma}^2(y)}\, dy, \\ \langle \hat{\mu}_\gamma, \varphi\rangle_{\Gamma_\gamma} &= \int\limits_0^1 \mu(y)\varphi(\gamma(y), y)\sqrt{1+\dot{\gamma}^2(y)}\, dy, \end{aligned} \tag{2.6}$$

holds for all $\varphi \in H^{1/2}_{00}(\Gamma_\gamma)$.

Theorem 2.1. *(*[KP1],[KP2]*) Let $f \in L^\infty(\hat{\Omega})$. Then $\gamma \mapsto J(\hat{u}_\gamma)$ is Fréchet differentiable in $\mathcal{S}$ and its derivative is characterized by*

$$D_\gamma J(\hat{u}_\gamma)\bar{\gamma} = \int_0^1 \mu(y)g(y)\bar{\gamma}(y)\, dy \tag{2.7}$$

for every $\bar{\gamma} \in H^3(0,1)$.

In (2.7) the functions μ and g depend on γ through (2.5) and (2.2). Thus the gradient of J can be expressed in terms of primal and dual variables of the chosen embedding domain technique. It can be viewed as an operator splitting method since it allows an expression of the gradient without explicit use of $\frac{\partial u}{\partial n}$ which is replaced by g. This has obvious numerical advantages since it can be costly to obtain reliable approximations to $\frac{\partial u}{\partial n}|\Gamma_\gamma$.

3. Mixed finite element approximation of $(\hat{P}_\gamma)$

For numerical realization of shape optimization problems the gradient computation plays a significant role. As already mentioned above for problems with Dirichlet boundary conditions normal derivatives of the state typically appear in the representation of the gradient [P]. Special attention is required to approximate the normal derivatives well numerically. In addition the cost functional is frequently not very sensitive with respect to Γ_γ so that small numerical errors may lead to wrong gradients. In the context of embedding domain methods for shape optimization, problems with multiple local minima as well as complete insensitivity of the cost with respect to Γ_γ (locking effect) were reported in [HJ, HN]. The main focus of the present note is therefore to demonstrate that the representation of the gradient in the form given by Theorem 2.1 is numerically effective.

For numerical realization we use a discretization of (2.2) based on two independent meshes: on the fictitious domain $\hat{\Omega}$ an equidistant mesh determined by N^2 interior meshpoints $(\xi_i, \eta_j) = (\frac{i}{N+1}, \frac{j}{N+1})$, $i, j = 1, \ldots, N$, is used. Elements $\hat{v}$ of $\hat{V}$ are approximated by bilinear tensor splines

$$\hat{v}^N(\xi, \eta) = \sum_{i,j=1}^{N} v_{ij}^N \varphi_i^N(\xi) \varphi_j^N(\eta),$$

where

$$\varphi_i^N(\xi) = \begin{cases} 1 - (N+1)|\xi - \xi_i|, & \text{for } \xi \in [\xi_{i-1}, \xi_i], \\ 0, & \text{else.} \end{cases}$$

The discretization of the interior boundary Γ_γ is given by M not necessarily equidistant interior meshpoints: $0 = y_0 < \cdots < y_{M+1} = 1$ and appropriate piecewise linear basis functions $\{\psi_i^M\}_{i=0}^{M+1}$

$$\gamma^M = \sum_{i=0}^{M+1} \gamma_i^M \psi_i^M.$$

Furthermore let $\{\chi_i\}_{i=1}^{M+1}$ denote the characteristic functions of the intervals $[y_{i-1}, y_i)$, $i = 1, \ldots, M+1$ and approximate the kernels g and μ in the representation (2.6) of $\hat{g}_\gamma$ and $\hat{\mu}_\gamma$ by

$$g^M = \sum_{i=1}^{M+1} g_i \chi_i \text{ and } \mu^M = \sum_{i=1}^{M+1} \mu_i \chi_i.$$

The spaces of all $\hat{v}^N$ and g^M are denoted by $\hat{V}^N$ and H^M respectively. Replacing in addition the curved boundary Γ_γ by a piecewise linear approximation Γ_{γ^M} one obtains the following approximation $\hat{g}^M_{\gamma^M}$ of $\hat{g}_\gamma$

$$\begin{aligned}\langle \hat{g}^M_{\gamma^M}, \tau_{\gamma^M} v^N \rangle_{\Gamma^M_\gamma} &= \sum_{i=1}^{M+1} g_i \int_{y_{i-1}}^{y_i} \hat{v}^N(\gamma^M(y), y)\sqrt{1 + (\dot{\gamma}^M)^2(y)}\, dy \\ &= G^M B^{N,M}_{\gamma^M} V^N,\end{aligned}$$

where G^M and V^N denote the coordinate vectors of $\hat{g}^M$ and $\hat{v}^N$ respectively, and $B^{N,M}_{\gamma^M} \in \mathbb{R}^{(M+1)\times N^2}$. Hence the discretizations of (2.2) as well as (2.5) are given by

$$\text{(3.1)} \qquad \begin{cases} a(\hat{u}^N, \hat{v}^N) + b^M(\hat{v}^N, \hat{g}^M_\gamma) = \langle F, \hat{v}^N \rangle_{V,V^*} \\ b^M(\hat{u}^N, \hat{w}^M) = 0, \end{cases}$$

for all $(\hat{v}^N, \hat{w}^M) \in \hat{V}^N \times H^M$ respectively. Above F stands either for $\tilde{f}_\gamma$ or for the distribution determined by $\tau_{\mathcal{C}} \hat{u}_\gamma - z$, and

$$b^M(\hat{v}^N, \hat{g}^M_{\gamma^M}) = \langle \hat{g}^M_{\gamma^M}, \tau_{\gamma^M} \hat{v}^N \rangle_{\Gamma^M_\gamma}.$$

System (3.1) can be expressed equivalently as

$$\text{(3.2)} \qquad \begin{pmatrix} L^N & (B^{N,M}_{\gamma^M})^T \\ B^{N,M}_{\gamma^M} & 0 \end{pmatrix} \begin{pmatrix} U^N \\ G^M \end{pmatrix} = \begin{pmatrix} F^{N,M}_{\gamma^M} \\ 0 \end{pmatrix},$$

with $L^N \in \mathbb{R}^{N^2 \times N^2}$ symmetric and positive definite. It follows that (3.2) is uniquely solvable if and only if ker $(B^{N,M}_{\gamma^M})^T = \{0\}$, or equivalently,

$$\text{(3.3)} \qquad b^M(\hat{v}^N, \hat{g}^M) = 0 \text{ for all } \hat{v}^N \text{ implies } \hat{g}^M = 0.$$

Next we show that condition (3.3) holds if the discretiztion for the interior boundary Γ_{γ^M} is not too fine compared to the grid on $\hat{\Omega}$.

Theorem 3.1. *If* $\min\{y_i - y_{i-1} \colon i = 1, \cdots, M+1\} > h = \frac{1}{M+1}$ *and* $M \geq N - 1$, *then condition* (3.3) *holds and the saddle point equation* (3.2) *is uniquely solvable.*

Proof. Note that (3.3) is equivalent to

$$\text{(3.4)}\qquad \begin{array}{l}\sum_{i=1}^{M+1} g_i \int_{y_{i-1}}^{y_i} \hat{v}^N(\gamma^M(y), y)\sqrt{1+(\dot{\gamma}^M)^2}\, dy = 0 \quad \text{for all } \hat{v}^N \\ \text{implies } G^M = 0.\end{array}$$

We shall show that $G^M = 0$ by using the following test functions:

$$\hat{v}_j^N(\xi,\eta) = \sum_{i=1}^{N} \varphi_i^N(\xi)\varphi_j^N(\eta), \quad \text{for } j = 1, \cdots, N.$$

These functions have the property that they are independent of ξ in a neighborhood of Γ_{γ^M}, in fact we have

$$\hat{v}_j^N(\xi,\eta) = \varphi_j^N(\eta), \quad \text{for } j = 1, \cdots, N, \xi \in [h, 1-h].$$

For the following argument we introduce the notation

$$\begin{aligned} \tilde{g}_j &= g_j\sqrt{1+(\dot{\gamma}^M)^2(y)} && \text{for } y \in (y_{j-1}, y_j), \\ \phi_j(\xi,\eta) &= \int_\xi^\eta \varphi_j^N(y)\, dy && j = 1, \cdots, M. \end{aligned}$$

Note that $\dot{\gamma}^M$ is constant on each subinterval (y_{j-1}, y_j).

Let us assume at first that $y_1 \geq 2h$. Setting $\hat{v}^N = \hat{v}_1^N = \varphi_1^N$ in (3.4) we find $g_1 = 0$. Proceeding by induction assume that $g_1 = \cdots = g_i = 0$ for some $i \in \{1, \cdots M\}$ and let $y_i \in [\tilde{j}h, (\tilde{j}+1)h)$. Then

$$\begin{aligned} b^M(\hat{g}^M, \varphi_j^N) &= \tilde{g}_i\phi_{\tilde{j}}\big((\tilde{j}-1)h, y_i\big) + \tilde{g}_{i+1}\phi_{\tilde{j}}\big(y_i, (\tilde{j}+1)h\big) \\ &= \tilde{g}_{i+1}\phi_{\tilde{j}}\big(y_i, (\tilde{j}+1)h\big) = 0 \end{aligned}$$

implies that $\tilde{g}_{i+1} = 0$ and hence $g_{i+1} = 0$. It follows that $G^M = 0$ if $y_1 \geq 2h$. Next we consider the case $y_1 \in (h, 2h)$. Let L be the minimal index such that $1 \leq L \leq M$ and

$$\begin{aligned} y_l &\in [lh, (l+1)h) \quad \text{for } l = 1, \cdots, L, \\ y_{L+1} &\geq (L+2)h. \end{aligned}$$

Evaluating (3.4) for $\hat{v}^N = v_j^N$, $j = 1, \cdots, L+1$ results in the following tridiagonal system

(3.5)

$$\begin{aligned} &\tilde{g}_1\phi_1(0, y_1) + \tilde{g}_2\phi_1(y_1, 2h) = 0 \\ &\tilde{g}_{j-1}\phi_j\big((j-1)h, y_{j-1}\big) + \tilde{g}_j\phi_j(y_{j-1}, y_j) + \tilde{g}_{j+1}\phi_j\big(y_j, (j+1)h\big) = 0, \\ &\tilde{g}_L\phi_L(Lh, y_L) + \tilde{g}_{L+1}\phi_L\big(y_L, (L+2)h\big) = 0, \end{aligned}$$

$j = 2, \cdots, L$. In case $L = 1$ the system consists of the first and third equations in (3.5) only. We argue that (3.5) is strictly diagonally dominant. In fact

$$\phi_j\big((j-1)h, y_{j-1}\big) + \phi_j\big(y_j, (j+1)h\big) = h - \int_{y_{j-1}}^{y_j} \varphi_j^N dy < \phi_j(y_{j-1}, y_j),$$

where the last inequality is a consequence of $y_j - y_{j-1} > h$, together with

$$\begin{aligned} &\frac{h}{2} + \phi_1(y_1, h) > \phi_1(y_1, 2h), \\ &\frac{h}{2} + \phi_{L+1}\big(y_L, (L+1)h\big) > \phi_{L+1}(y_L, Lh) \end{aligned}$$

imply the desired diagonal dominancy. Consequently (3.5) has only the trivial solution and thus $g_j = 0$ for $j = 1, \cdots, L+1$. If $L = M$ the proof is complete. Otherwise we proceed by induction as in the second part of the case $y_1 \geq 2h$ to obtain $G^M = 0$. □

For $M \geq N$ condition (3.3) need not be satisfied. Consider, for example, $\Gamma = \{\gamma_0\} \times (0,1)$ for some $\gamma_0 \in (0,1)$. In this case (3.3) yields N equations for $M+1$ unknowns and (3.1) has infinitely many solutions.

To specify the finite dimensional optimization problem we define

$$\mathcal{S}^M = \{\gamma^M = \sum_{i=0}^{M+1} \gamma_i^M \psi_i^M \colon \mu \leq \gamma^M(y) \leq \nu\},$$

and consider

$$(\hat{P}_\gamma^N) \qquad \begin{aligned} &\min J(\hat{u}_{\gamma^M}^N) \quad \text{over } \gamma^M \in \mathcal{S}^M \\ &\text{subject to } \hat{u}_{\gamma^M}^N \text{ solution of (3.1) with } F = \tilde{f}_{\gamma^M}. \end{aligned}$$

For numerical purposes we approximate the gradient of $\gamma^M \to J(\hat{u}_{\gamma^M}^N)$ by the discretization of the gradient of $\gamma \to J(\hat{u}_\gamma)$, i.e. we take for $\bar{\gamma}^M = \sum_{i=0}^{M+1} \bar{\gamma}_i^M \psi_i^M$

$$D_{\gamma^M} J(\hat{u}_{\gamma^M}^N)\bar{\gamma}^M \mathrel{\widehat{=}} \int_0^1 g_{\gamma^M}^M(y)\, \mu_{\gamma^M}^M(y)\, \bar{\gamma}^M(y)\, dy, \tag{3.6}$$

where $(\hat{u}_{\gamma^M}^N, \hat{g}_{\gamma^M}^M)$ is the solution to (3.1) with $F = \tilde{f}_{\gamma^M}$, $(\hat{\lambda}_{\gamma^M}^N, \hat{\mu}_{\gamma^M}^M)$ is the solution to (3.5) with $\langle F, \hat{v}^N \rangle_{\hat{V}^*, V} = \int_{\mathcal{C}} (\tau_{\mathcal{C}} \hat{u}_{\gamma^M}^N - z)\hat{v}^N\, ds$, and $g_{\gamma^M}^M, \mu_{\gamma^M}^M$ are defined as in (2.6).

4. Schur complement realization

Every iterative technique to solve $(\hat{P}_\gamma^N)$ depends on numerous solutions of (3.1) for different γ^M. In this section we therefore describe an efficient way to solve (3.1). It will be convenient to drop the superscripts and to write B_{γ^M}, L, F_{γ^M}, ... for $B_{\gamma^M}^{N,M}$, L^N, $F_{\gamma^M}^{N,M}$. Theorem 3.1 implies invertibility of the Schur complement $B_{\gamma^M} L^{-1} (B_{\gamma^M})^T$. Consequently the solution of (3.2) is given by

$$G = (B_{\gamma^M} L^{-1} B_{\gamma^M}^T)^{-1} B_{\gamma^M} L^{-1} F_{\gamma^M} \tag{4.1}$$

$$U = -L^{-1}(B_{\gamma^M}^T G + F_{\gamma^M}) \tag{4.2}$$

Since (4.1)–(4.2) must be evaluated frequently during the course of the optimization and since L is independent of γ^M the first step consists in a Cholesky factorization of L so that

$$L = R^T R,$$

for some upper triangular matrix $R \in \mathbb{R}^{N^2 \times N^2}$.
The Schur complement can thus be represented in the form

$$B_{\gamma^M} L^{-1} B_{\gamma^M}^T = Y^T Y,$$

where $Y = R^{-T} B_{\gamma^M}^T \in \mathbb{R}^{N^2 \times (M+1)}$. This suggests the following algorithm to solve (4.1)–(4.2).

Algorithm
Solve successively for (y, z, Y, G, y, U):

$$\begin{aligned}
&R^T y = F_{\gamma^M} \\
&Rz = y \qquad (\text{ thus } z = L^{-1} F_{\gamma^M}) \\
&R^T Y = B_{\gamma^M}^T \\
&Y^T Y G = B_{\gamma^M} z \\
&R^T y = -B_{\gamma^M}^T G + F_{\gamma^M} \\
&RU = y.
\end{aligned}$$

The Algorithm requires 2 forward and $M+3$ backward substitutions involving the $N^2 \times N^2$-matrix R and the linear system solve involving the $(M+1) \times (M+1)$ matrix $Y^T Y$. Compared to the dimension of the system (4.1)–(4.2) which is $(N^2 + (M+1))^2$ the Algorithm represents a significant computational reduction. We demonstrate this fact also by a numerical test. In Table 1 we specify the computing times on a PC-Pentium 200 for solving (4.1)–(4.2) for various choices of N with $N = 2M$. The second column contains the times required for the Cholesky factorization, the third column the times required for the

X	Cholesky	Algor	direct
10			0.05
20	0.06	0.04	0.28
30	0.15	0.22	1.09
40	0.44	0.48	2.63
50	0.93	1.04	5.86
60	1.48	2.19	9.11
70	2.42	4.01	11.97
80	4.05	6.10	18.77
90	7.64	9.66	25.32

TABLE 1. Comparison of CPU time

Algorithm and the last column the computing time required by the MATLAB linear equation solver to solve directly (4.1)–(4.2). If (4.1)–(4.2) needs to be solved several times with different γ^M and $F^{N,M}_{\gamma^M}$, the time required for the Cholesky factorization must be considered only once.

In the discussion of the approximation of (2.5) by (4.1)–(4.2) we left out so for the delicate question of how to realize numerically the extension by zero of f_γ. Since Γ_{γ^M} will not coincide with a grid line corresponding to the grid of the bilinear tensor splines the discretization of $\tilde{f}_\gamma$ requires a compromise which adversely effects the accuracy of the approximation of (2.5) by (4.1)–(4.2). In the case that Ω is one dimensional we carried out very detailed numerical tests of the advantages that arise from calculating $(\tilde{f}_{\gamma^M}, \hat{v}^N)_{L^2(\hat{\Omega})}$ precisely, even if Γ_{γ^M} does not coincide with gridpoints of the grid for $\hat{v}^N$. We found no significant influence due to the type of extension on the rate of convergence of $(\hat{u}^N_{\gamma^M}, \hat{g}^M_{\gamma^M})$. In the two dimensional case we simply set zero those coordinates of $\tilde{f}_{\gamma^M}$ corresponding to nodes in the fictitious domain. Let us point out that an extension of f_γ as continuous function onto $\hat{\Omega}$ results in $\hat{g}^N$ which is not any more related to $\frac{\partial u^N_\gamma}{\partial n}$. Extension of f_γ by zero is easier to implement and gives better approximation to u_γ than extension of f_γ by zero. Consequently we solved the Algorithm for F_{γ^M} arising from f_γ both from extension by zero and by extension as continuous function. The former was used to approximate $\frac{\partial u}{\partial n}|\Gamma_\gamma$ via $g^N_{\Gamma^M_\gamma}$, the latter to approximate u_γ. This procedure lead to a considerable improvement of the accuracy of the approximation of u_γ by U at the only additional cost of two forward and two backward substitutions involving the continuous extension of f_γ.

Let us close this section by recalling that it was proved in [GR] that $(\hat{u}^N_{\gamma^M}, \hat{g}^M_{\gamma^M})$ converges to $(\hat{u}_{\gamma^M}, \hat{g}_{\gamma^M})$ as $N \to \infty$ if the Babuska Brezzi condition is satisfied. For a problem similar to (2.1) this was satisfied for the choice $N = 3M$, [GG]. In our computations we observed strong oszillations of $\hat{g}^M_{\gamma^M}$, as long as the discretization of $\Gamma^M_{\gamma^M}$ was too fine compared to the grid of Ω. The ratio $N\colon M = 2\colon 1$ turned out to be a reasonable compromise between feasability of $\hat{g}^M_{\gamma^M}$ and the dimension of the system (3.2) at a given resolution of $\Gamma^M_{\gamma^M}$.

5. Applications

In this section we address numerical issues related to the embedding domain based approach to solve shape optimization problems. First of all we demonstrate the efficiency of the gradient given by (3.6) by means of two examples for which the analytical gradient is known explicitly. We also point out by means of a one dimensional example that it is advisable to numerically calculate the gradient by discretizing the analytical gradient of the infinite dimensional problem as given by (3.6). In fact, numerical artifacts may lead to useless gradients if they are calculated as exact gradients of the discretized problems. Finally we address the effects of different implementations of the "extension by zero" involved in $\tilde{f}_\gamma$ if Γ_γ does not coincide with a node of the discretization for the state variable.

5.1. **Example 1:** This is an adaptation from a one-dimensional example already treated in [HJ]. The state equation is given by the 2-point boundary value problem

$$\begin{aligned} -u'' &= f \qquad \text{on } (0,\gamma) \\ u(0) &= u(\gamma) = 0 \end{aligned} \tag{5.1}$$

with $f \in \mathbb{R}$ and $\gamma \in (\frac{1}{2}, \frac{3}{2})$. Its solution is given by

$$u_\gamma(x) = \frac{f}{2} x(\gamma - x), \qquad \text{for } x \in (0,\gamma).$$

As a cost we choose

$$J(\gamma) = \big(u_\gamma(\xi) - z\big)^2. \tag{5.2}$$

The numerical results presented below are based on $f = 2$, $\xi = \frac{1}{2}$, $z = u_{\gamma^*}(\xi)$ and $\gamma^* = 1.2$. It will be convenient to introduce

$$\rho = 2(u_\gamma(\xi) - z).$$

The gradient of J with respect to $\gamma \in \mathbb{R}$ is given by

$$DJ(\gamma) = \big(\frac{\rho}{2}\big) f \xi. \tag{5.3}$$

The dual equation associated with (2.1) is given by

$$\begin{aligned} \lambda'' &= \rho\delta(\xi) \qquad \text{on } (0,\gamma) \\ \lambda(0) &= \lambda(\gamma) = 0 \end{aligned} \tag{5.4}$$

Its solution can be expressed as

$$\lambda_\gamma(x) = \begin{cases} (\frac{\xi}{\gamma} - 1)\rho x & 0 \le x < \xi, \\ (\frac{x}{\gamma} - 1)\rho\xi & \xi \le x \le \gamma. \end{cases}$$

One verifies the relationship

$$DJ(\gamma) = -u'_\gamma(\gamma)\lambda'_\gamma(\gamma). \tag{5.5}$$

Extending (5.1) and (5.4) to $\hat{\Omega} = (0,2)$ one obtains the equivalent embedding domain systems in $H^1_0(0,2) \times \mathbb{R}$

$$\begin{aligned} &(\hat{u}', \hat{v}')_{\hat{\Omega}} - \hat{g}\hat{v}(\gamma) = (f, \hat{v})_{(0,\gamma)}, \qquad \hat{v} \in H^1_0(0,2) \\ &\hat{u}(\gamma) = 0 \end{aligned} \tag{5.6}$$

respectively

$$\begin{aligned} &(\hat{\lambda}', \hat{v}')_{\hat{\Omega}} - \hat{\mu}\hat{v}(\gamma) = -\rho\hat{v}(\xi), \qquad \hat{v} \in H^1_0(0,2) \\ &\hat{\lambda}(\gamma) = 0. \end{aligned} \tag{5.7}$$

Discretizing the primal equation (5.6) on the uniform grid $x_i = 2i/(N+1) = ih$, $i = 1, \cdots, N$ using piecewise linear splines φ_i one obtains the linear system analogous to (3.2)

$$\begin{pmatrix} D & B^T \\ B & 0 \end{pmatrix} \begin{pmatrix} U \\ G \end{pmatrix} = \begin{pmatrix} F \\ 0 \end{pmatrix} \tag{5.8}$$

where the matrices $L \in \mathbb{R}^{N\times N}$ and $B \in \mathbb{R}^{1\times N}$ are determined by

$$L = \frac{1}{h}\begin{pmatrix} 2 & -1 & & & \\ -1 & 2 & -1 & & \\ & \ddots & \ddots & \ddots & \\ & & -1 & 2-1 & \\ & & & -1 & 2 \end{pmatrix}, \quad B^T = -\begin{pmatrix} \varphi_1(\gamma) \\ \vdots \\ \varphi_N(\gamma) \end{pmatrix}.$$

Let

$$\gamma \in [x_\sigma, x_{\sigma+1})$$

for some $1 < \sigma < N$ then the coordinates of $F \in \mathbb{R}^N$ are given by

$$F_i = \begin{cases} fh & i = 1, \cdots, \sigma - 1 \\ f\int_{x_{\sigma-1}}^{\gamma} \varphi_\sigma \, dx & i = \sigma \\ f\int_{x_\sigma}^{\gamma} \varphi_{\sigma+1} \, dx & i = \sigma + 1 \\ 0 & \text{else.} \end{cases} \tag{5.9}$$

In the following proposition we shall treat the special case where γ and ξ coincide with gridpoints, i.e.

$$\gamma = x_\sigma \quad \text{and} \quad \xi = x_\tau \tag{5.10}$$

for some $0 < \tau < \sigma < N$.

Proposition 5.1. *Let $(\hat{u}^N, \hat{g}^N)$ and $(\hat{\lambda}^N, \hat{\mu}^N)$ with $\hat{u}^N = \sum_{i=1}^N u_i\varphi_i$ and $\hat{\lambda}^N = \sum_{i=1}^N \lambda_i\varphi_i$ denote the solutions of discretizations of* (5.6) *and* (5.7) *by linear splines and assume that* (5.10) *holds. Then $\hat{u}^N$ and $\hat{\lambda}^N$ coincide with the linear interpolant of $\hat{u}_\gamma$ and $\hat{\lambda}_\gamma$, and furthermore $\hat{g}^N = u_\gamma'(\gamma)$, and $\hat{\lambda}^N = \lambda_\gamma'(\gamma)$. Therefore the numerical gradient $-\hat{g}^N\hat{\lambda}^N$ coincides with* (5.3).

Proof. Since $\gamma = x_\sigma$ we have $B^T = \hat{e}_\sigma$ where $\hat{e}_\sigma$ denotes the σ-th canonical basis vector of $\mathbb{R}^N$.

As a consequence the last equation in (5.8) gives

$$u_\sigma = 0, \tag{5.11}$$

where we put $U = \text{col}(u_1, \cdots, u_N)$. Partitioning

$$U = \begin{pmatrix} w \\ v \end{pmatrix}, \quad \hat{e}_\sigma = \begin{pmatrix} e_\sigma \\ 0 \end{pmatrix}, \quad F = \begin{pmatrix} F^\sigma \\ 0 \end{pmatrix},$$

with w, e_σ, $F^\sigma \in \mathbb{R}^\sigma$ and $v \in \mathbb{R}^{N-\sigma}$ the first with N equations in (5.8) are equivalent to

$$\frac{1}{h}\begin{pmatrix} L_\sigma & C_\sigma^T \\ C_\sigma & L_{N-\sigma} \end{pmatrix}\begin{pmatrix} w \\ v \end{pmatrix} - G\begin{pmatrix} e_\sigma \\ 0 \end{pmatrix} = \begin{pmatrix} F^\sigma \\ 0 \end{pmatrix}. \tag{5.12}$$

The matrices L_σ, $L_{N-\sigma}$ and C_σ are obtained by partitioning L according to the partition of U. In view of

$$w_\sigma = 0$$

one concludes

$$C_\sigma w = 0$$

and consequently

$$L_{N-\sigma} v = 0$$

which by regularity of $L_{N-\sigma}$ implies that

$$v = 0.$$

Therefore w satisfies

$$\frac{1}{h} L_\sigma w - G e_\sigma = F^\sigma. \tag{5.13}$$

Note that the first $(\sigma - 1)$ equations in (5.13) are identical to the equations derived by applying central differences to (5.1). Since the central difference approximation of the second derivative on a uniform grid is exact for polynomials of degree up to two w is given by

$$w_i = u_\gamma(x_i), i = 1, \cdots, \sigma - 1. \tag{5.14}$$

Solving the last equation in (5.13) for G yields

$$G = -F_\sigma^\sigma - \frac{1}{h} w_{\sigma-1}, \tag{5.15}$$

which together with (5.14), (5.9) and (5.10) results in

$$G = -\frac{f}{2} h - \frac{f}{2h} (\sigma - 1) h^2 = -\frac{f}{2}\gamma,$$

and therefore

$$G = u_\gamma'(\gamma).$$

Next we use the assumption that ξ coincides with a gridpoint as well. The analog to system (5.13) is found to be

$$\frac{1}{h} L_\sigma \ell - \mu e_\sigma = d^\sigma, \tag{5.16}$$

where $\ell = \operatorname{col}(\lambda_1, \cdots, \lambda_N)$ and

$$d^\sigma = \rho e_\tau.$$

One verifies that the first $(\sigma - 1)$ equations of (5.16) satisfy

$$\begin{aligned} \lambda_i &= i\lambda_1, && 1 \le i \le \tau \\ \lambda_{\tau+i} &= i\rho h + (\tau + i)\lambda_1 && 1 \le i \le \sigma - \tau. \end{aligned}$$

The constraint $\lambda_\sigma = 0$ yields

$$\lambda_1 = -(1 - \frac{\tau}{\sigma})\rho h,$$

which results in

$$\begin{aligned} \lambda_i &= -(1 - \frac{\tau}{\sigma})\rho x_i, && 1 \le i \le \tau \\ \lambda_{\tau+i} &= -(1 - \frac{\tau}{\sigma})\rho x_{\tau+i} + (x_{\tau+i} - \xi)\rho && 1 \le i \le \sigma - \tau. \end{aligned}$$

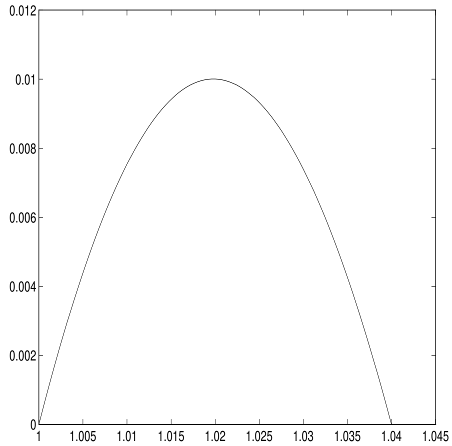

FIGURE 1. $|\hat{u}_a^N - u_a|_{\infty,[0,a]}$

The last equation in (5.16) gives

$$\begin{aligned}\mu &= -\frac{1}{h}\lambda_{\sigma-1}\\ &= -\frac{1}{h}[-(1-\frac{\tau}{\sigma})(\sigma-1)+(\sigma-1-\tau)]\rho h = \frac{\tau}{\sigma}\rho = \frac{\xi}{\gamma}\rho,\end{aligned}$$

and therefore

$$\mu = \lambda'_\gamma(\gamma).$$

This concludes the proof. □

If the location of the internal boundary does not match a grid point $w_\sigma = 0$ will in general not be satisfied. Consequently (5.8) cannot be reduced to (5.13) and the previous argument breaks down. Figure 1 shows the approximation error $|\hat{u}_\gamma^N - u_\gamma|_{\infty,[0,\gamma]}$ for $N = 49$ as γ varies in $[\gamma_0, \gamma_1] = [1, \frac{26}{25}]$ (note $\gamma_0 = 25h$ and $\gamma_1 = 26h$).

According to Proposition 5.1 the error vanishes at γ_0 and γ_1. It attains its maximum when the internal boundary lies exactly between two gridpoints. In this latter case we observed only linear convergence of $\hat{u}_\gamma^N$ to $\hat{u}_\gamma$ as $h \to 0$. This illustrates the strong dependence of the quality of approximation on a. Figure 2 demonstrates the consequences of this dependence of accuracy of the approximation of $\hat{u}_\gamma^N$ to $\hat{u}_\gamma$ to the discretized cost when γ is increased from $\gamma = 1$ to $\gamma = 1.5$ with stepsize $\delta\gamma = 0.005$. The solid (dotted) linestyles refer to the discretized (exact) cost, the asterisks indicate the underlying computational grid. The degradation of the quality of approximation of $\hat{u}_\gamma$ by $\hat{u}_\gamma^N$ when γ moves away from the gridpoints causes a nonsmooth behavior of the

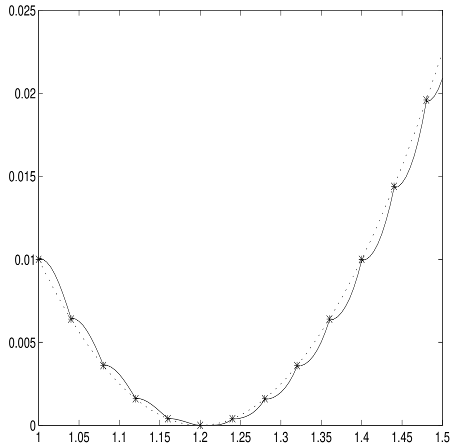

FIGURE 2. The discretized cost

discretized cost. Obviously, it would be difficult for any gradient based optimization algorithm to find the global minimum using derivative information from the discrete model. Figure 3 compares a forward difference approximation to the derivative of the discretized cost (with stepsize $\delta_\gamma/5$) to the exact derivative of J. Again asterisks denote the computational gridpoints. Note the lack of sensitivity and differentiability of the cost near the grid. Using backward or central differences leads to the same types of graphs. The representation based on Theorem 2.1. of DJ provides a much better approximation of the derivative of J. This is illustrated in Figure 4.

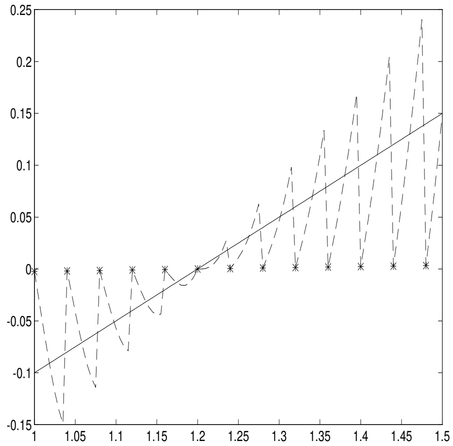

FIGURE 3. A forward difference approximation to DJ

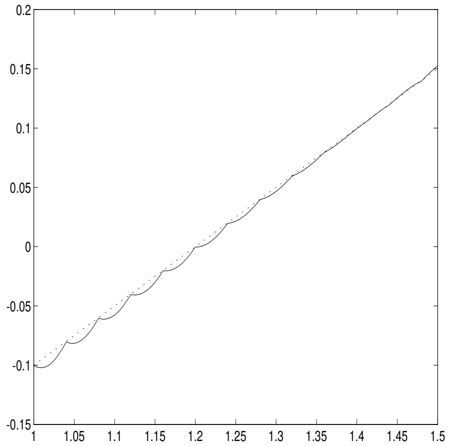

FIGURE 4. The approximation of DJ based on (2.6)

linestyle	F^σ_σ, $F^\sigma_{\sigma+1}$
solid	$F^\sigma_\sigma = f\int_{x_{\sigma-1}}^{\gamma} \varphi_\sigma\, dx,\ F^\sigma_{\sigma+1} = 0$
dash	$F^\sigma_\sigma = f\int_{x_{\sigma-1}}^{\gamma} \varphi_\sigma\, dx,\ F^\sigma_{\sigma+1} = f\int_{x_\sigma}^{\gamma} \varphi_{\sigma+1}\, dx,$
dot	$F^\sigma_\sigma = f\int_{x_{\sigma-1}}^{x_{\sigma+1}} \varphi_\sigma\, dx,\ F^\sigma_{\sigma+1} = 0$
dashdot	$F^\sigma_i = \gamma h,\ i \geq 1$

TABLE 2. Convergence rate

We conclude the discussion of this example with a few comments on the effect of different numerical realizations of the extension of f into Ω. If $\gamma = 1$ coincides with x_σ for some $1 \leq \sigma \leq N$ one has $F^\sigma_i = 0$ for $i \geq \sigma$. Hence the choice of F^σ_σ only affects G via (5.15). The effect of different strategies to approximate $\tilde{f}^M_\gamma$ in the worst case when γ lies exactly between two gridpoints is documented in Figure 5 which shows $|\hat{u}^N_\gamma - u_\gamma|_{\infty,[0,\gamma]}$ versus the meshsize $h = \frac{2}{N+1}$ as N is increased in steps of 4 from 10 to 100. Table 2 explains the types of approximations that are used for $\tilde{f}^M_\gamma$ in Figure 5.

The approximation indicated by dashdots corresponds to a continuous extension of f across the internal boundary. It serves as a reference for the remaining three curves which realize different extensions by zero of f onto $\Omega\backslash\Omega_\gamma$. Figure 5 clearly indicates that the particular technique to approximate $\tilde{f}_{\gamma^M}$ only influences the size of the error $|\hat{u}^N_\gamma - u_\gamma|_{\infty,[0,\gamma]}$ and does not improve the rate of convergence: for all variants one observes linear convergence. In view of this observation it is doubtful

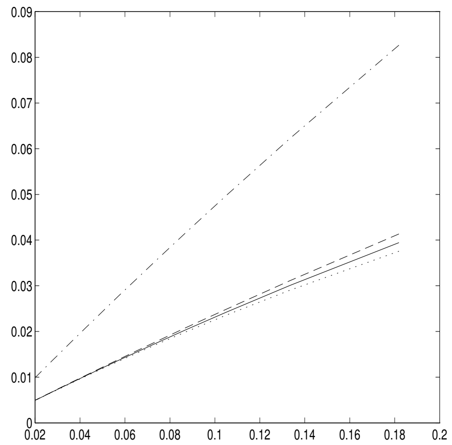

FIGURE 5. Rate of convergence for $|\hat{u}_a^N - u_a|_{\infty,[0,a]}$

whether it is worthwhile to apply the second and third type of approximation which are more time consuming in higher dimensions.

5.2. **Example 2:** This is a two dimensional example with known analytical solution. In order to construct such an example, (2.1) is modified to allow for inhomogeneities which are themselves dependent on γ.

For $\gamma \in \mathcal{S}$ and $(x, y) \in \hat{\Omega}$ consider

$$\hat{u}_\gamma(x, y) = \sin \pi y \sin \pi \frac{x(x - \gamma(y))}{1 - \gamma(y)}$$

and observe that $\tau_\gamma \hat{u}_\gamma = 0$. Hence we have

$$\begin{aligned} &\hat{u}_\gamma \in H_0^1(\hat{\Omega}) \cap C^2(\bar{\hat{\Omega}}) \\ &u_\gamma = \hat{u}_\gamma|_{\Omega_\gamma} \in H_0^1(\Omega_\gamma) \cap C^2(\bar{\Omega}_\gamma). \end{aligned}$$

Defining

$$f_\gamma = -\Delta \hat{u}_\gamma \in C(\bar{\hat{\Omega}})$$

$\hat{u}_\gamma$ satisfies (P_γ) on Ω_γ as well as on $\hat{\Omega}$. Clearly $\gamma \to \hat{u}_\gamma$ is differentiable which entails that

$$D_\gamma J(\hat{u}_\gamma)\bar{\gamma} = 2(\tau_{\mathcal{C}} \hat{u}_\gamma - z, \tau_{\mathcal{C}}(D_\gamma \hat{u}_\gamma \bar{\gamma}))_{\mathcal{C}}. \tag{5.17}$$

Furthermore one verifies for this example that

$$\sqrt{1 + \dot{\gamma}^2}\, \tau_\gamma(D_\gamma(\hat{u}_\gamma)\bar{\gamma}) = \frac{\partial u_\gamma}{\partial n}\, \bar{\gamma}. \tag{5.18}$$

Proceeding formally one obtains

$$\Delta(D_\gamma \hat{u}_\gamma \bar{\gamma}) = -D_\gamma f_\gamma \bar{\gamma}.$$

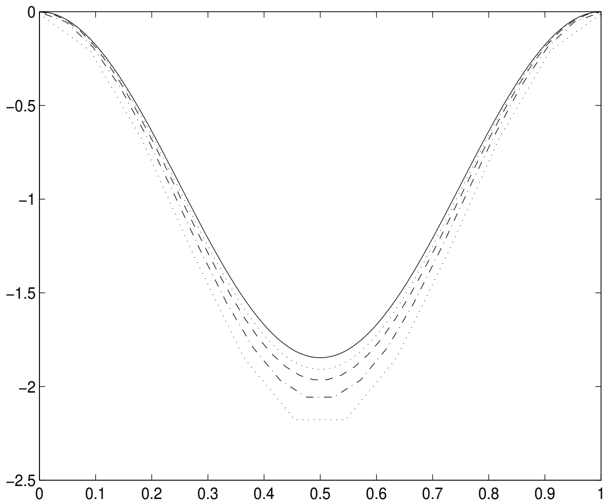

FIGURE 6. Approximation of the gradient of J

Taking the inner product with $\hat{\lambda}_\gamma$ and using $D_\gamma u_\gamma \bar{\gamma} \in H_0^1(\hat{\Omega})$ as test-function in the dual equation (2.5) leads to

$$\begin{aligned}(D_\gamma f_\gamma \bar{\gamma}, \hat{\lambda}_\gamma)_{\hat{\Omega}} &= (-\Delta(D_\gamma \hat{u}_\gamma \bar{\gamma}), \hat{\lambda}_\gamma)_{\hat{\Omega}} = (\nabla(D_\gamma \hat{u}_\gamma \bar{\gamma}), \nabla \hat{\lambda}_\gamma)_{\hat{\Omega}} \\ &= -2(\tau_{\mathcal{C}} \hat{u}_\gamma - z)\tau_{\mathcal{C}}(D_\gamma \hat{u}_\gamma \bar{\gamma}))_{\mathcal{C}} + \langle \hat{\mu}_\gamma, \tau_\gamma(D_\gamma \hat{u}_\gamma \bar{\gamma})\rangle,\end{aligned}$$

which by (5.17) and (5.18) is equivalent to

$$\begin{aligned}D_\gamma J(\hat{u}_\gamma)\bar{\gamma} &= \int_0^1 \mu_\gamma(y) \frac{\partial u_\gamma}{\partial n}(y)\bar{\gamma}(y)\, dy - (D_\gamma f_\gamma \bar{\gamma}, \hat{\lambda}_\gamma)_{\hat{\Omega}} \\ &= \int_0^1 \mu_\gamma(y) g_\gamma(y) \bar{\gamma}(y)\, dy - (D_\gamma f_\gamma \bar{\gamma}, \hat{\lambda}_\gamma)_{\hat{\Omega}}.\end{aligned}$$

The additional term on the righthand side above is due to the fact that in this example f_γ depends on γ. Since the lefthand side and $D_\gamma f_\gamma \bar{\gamma}$ are explicitly known this example provides a means to demonstrate the convergence of the discretized gradient. Figure 6 shows the Riesz representors of $D_\gamma J(\hat{u}_{\gamma^*})$ (solid) and of $\int_0^1 g^M_{\gamma^M}(y)\mu^M_{\gamma^M}(y)\bar{\gamma}(y)\, dy - (D_\gamma f_\gamma \bar{\gamma}, \hat{\lambda}_\gamma)_{\hat{\Omega}}$ for $M = 10,\ 20,\ 40,\ 80$ with $\gamma^* \equiv 0.6$ and $\mathcal{C} = \{0.8\} \times (0, 1)$.

REFERENCES

[BF] F. Brezzi and M.Fortin: *Mixed and Hybrid Finite Element Methods* Springer, New York, 1991.

[DZ] M.C. Delfour and J.-P. Zolesio: *Velocity method and Lagrange formulation for the computation of the shape Hessian*, SIAM Journal on Control and Optimization **29**, (1991), 1414–1442.

[GG] V. Girault and R. Glowinski: *Error analysis of a fictitious domain method applied to a Dirichlet problem,* Japan Journal of Industrial and Applied Mathematics, **12** (1995), 487–514.

[GPP] R. Glowinski, T–W. Pan and J. Periaux: *A fictitious domain method for Dirichlet problem and applications*, Comp. Methods in Appl.Mech. and Eng. **111** (1994), 283–303.

[GR] Ch. Großmann and H. Roos: *Numerik Partieller Diffrentialgleichungen,* B.G. Teubner , Stuttgart, 1994.

[HJ] J. Haslinger and D. Jedelský *Genetic algorithms and fictitious domain based approaches in shape optimization*, to appear in Struct.Opt.

[HN] J. Haslinger and P. Neittaanmäki: *Finite Element Approximation for Optimal Shape Design: Theory and Applications*, J. Wiley, Chichester, 1988.

[KP1] K. Kunisch and G. Peichl: *Shape optimization for mixed boundary value problems based on an embedding domain method*, to appear in DCDIS

[KP2] K. Kunisch and G. Peichl: *Embedding domain technique based representation of the gradient for some shape optimization problems*, to appear in Advances in Mathematical Sciences and Applications.

[P] O. Pironneau: *Optimal shape Design for Elliptic Systems,* Springer, Berlin, 1984.

K.K. and G.P.:Institut für Mathematik, Karl-Franzens-Universität Graz, Heinrichstrasse 36, A-8010 Graz